

# Nucleon Structure and Generalized Parton Distributions

**Eric Voutier**

Laboratoire de Physique Subatomique et de Cosmologie  
IN2P3-CNRS / Université Joseph Fourier  
53 avenue des Martyrs  
38026 Grenoble cedex, France

## **Abstract.**

This paper discusses a selected part of the experimental program dedicated to the study of Generalized Parton Distributions, a recently introduced concept which provides a comprehensive framework for investigations of the partonic structure of the nucleon. Particular emphasis is put on the Deeply Virtual Compton Scattering program performed at the Jefferson Laboratory. The short and long term future of this program is also discussed in the context of the several experimental efforts aiming at a complete and exhaustive mapping of Generalized Parton Distributions.

## **1 Introduction**

From an experimental point of view, the story of the nucleon structure started in the fifties when deviations from the Mott cross section were observed in elastic electron scattering, meaning that the nucleon was no longer a pointlike object [1]. The size of the nucleon is embedded in the so-called electromagnetic form factors which characterize the nucleon shape with respect to the electromagnetic interaction. This shape depends on the resolution of the probe which is controlled by the momentum transfer  $Q^2$  to the nucleon, and which can also be seen as the size of the volume to which the virtual photon couples. This leads to the non-relativistic picture of the form factors as Fourier transforms of the charge and magnetisation densities of the nucleon.

At the end of the sixties, an unexpected result was obtained in Deep Inelastic electron Scattering (DIS) where it was found that the cross section for excitation energies well beyond the resonance region was weakly depending on the momentum transfer as compared to elastic scattering [2]. This behaviour was later

identified as the first evidence of the existence of quarks. The cross section for these experiments depends on the additional variable  $x_B$ , that is the fraction of the nucleon longitudinal momentum carried by the quarks, and can be expressed in terms of the probability to find in the nucleon a parton of given longitudinal momentum. This feature led to extensive measurements of momentum and spin distributions of quarks into polarized and unpolarized nucleons, the so-called parton distributions whose satisfactory knowledge has now been obtained after thirty years of experimental efforts.

However, the puzzle of the spin structure of the nucleon is not yet resolved. DIS experiments determined the contribution of the quarks spin to the nucleon spin to amount only to 20-30 % of the total spin [3]. This surprising result suggests that the gluons spin may play a significant role in this problem. The recent results of the COMPASS experiment do not support this hypothesis [4]. What is the origin of the nucleon spin and what is the importance of orbital momentum are still unanswered questions. The Generalized Parton Distribution (GPD) framework can contribute to this problem within a comprehensive picture that unifies form factors, parton distributions, and the total angular momentum of quarks.

The next section introduces the general concept of GPDs and some remarkable properties that link GPDs to the usual observables of the nucleon structure. The experimental access to GPDs is then discussed in the context of the Deeply Virtual Compton Scattering (DVCS) process. Recent results from Jefferson Laboratory (JLab) experiments are further presented before addressing briefly the forthcoming experimental programs at the different lepton facilities.

## 2 Generalized Parton Distributions

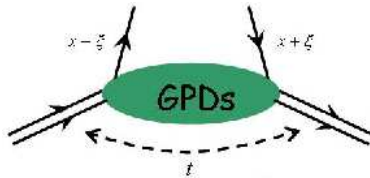


Figure 1. Symbolic representation of GPDs.

GPDs are four universal functions ( $H^q$ ,  $E^q$ ,  $\tilde{H}^q$ , and  $\tilde{E}^q$  where  $q$  denotes the quark flavor) describing the non-perturbative quark structure of the nucleon (correspondingly four gluon GPDs describe the gluon structure) [5–7]. They correspond to the overlap probability  $\Psi^*(x - \xi) \cdot \Psi(x + \xi)$  of picking a quark in the nucleon and inserting it back with a different (or same) spin, longitudinal momentum, and transverse position (fig. 1). GPDs depend on three parameters:  $x$  the initial longitudinal momentum of the quark,  $\xi$  the transferred longitudinal momentum or skewness parameter, and  $t$  the momentum transfer to the nucleon

that can be interpreted as the Fourier conjugate of the transverse position in the impact parameter space [8]. The richness of the GPDs parametrization of the nucleon sub-structure is in their non-diagonal feature which, among others, allows for initial nucleon spin-flip, a source of information which is not accessible with DIS. A simple physics picture [8–11] has been proposed which allows to interpret GPDs as the  $1/Q$  resolution distribution in the transverse plane of partons with longitudinal momentum  $x$ , constituting a femto-tomography of the nucleon.

The optical theorem provides a link between the forward limit of the Compton scattering amplitude and DIS, leading to the relations between GPDs and parton distributions

$$H^q(x, \xi = 0, t = 0) = q(x) \quad \tilde{H}^q(x, \xi = 0, t = 0) = \Delta q(x) \quad . \quad (1)$$

The first moment of each GPD identifies to a distinct form factor of the nucleon:

$$\int_{-1}^{+1} dx H^q(x, \xi, t) = F_1^q(t) \quad \int_{-1}^{+1} dx \tilde{H}^q(x, \xi, t) = g_A^q(t) \quad (2)$$

$$\int_{-1}^{+1} dx E^q(x, \xi, t) = F_2^q(t) \quad \int_{-1}^{+1} dx \tilde{E}^q(x, \xi, t) = g_P^q(t) \quad (3)$$

where the  $\xi$  independence results from Lorentz invariance. The second moment of  $H$  and  $E$  GPDs are linked together within Ji's sum rule [7] to the total angular momentum of quarks:

$$J^q = \frac{1}{2} \Delta \Sigma + L^q = \frac{1}{2} \int_{-1}^{+1} dx x [H^q(x, \xi, t = 0) + E^q(x, \xi, t = 0)] \quad . \quad (4)$$

This last expression has generated a lot of interest: considering that DIS provides the spin part of the angular momentum, the knowledge of  $H$  and  $E$  GPDs allows to access the quark orbital momentum.

### 3 Deeply Virtual Compton Scattering

GPDs can experimentally be accessed in exclusive leptonproduction of photons and mesons. The latter case, where the GPD information is convoluted with a distribution amplitude describing the out-going meson, and which requires the selection of longitudinal virtual photons is not discussed here. A comprehensive review can be found in [12].

DVCS, corresponding to the absorption of a virtual photon by a nucleon followed quasi-instantaneously by the emission of a real photon (fig. 2), is the simplest reaction which allows access to GPDs. This process became very important for nucleon structure studies when it was shown that, in the Bjorken limit, the leading contribution to the reaction amplitude could be represented by the so-called handbag diagram (fig. 2). The important feature of this representation is the factorization [13, 14] of the reaction amplitude in a known hard part

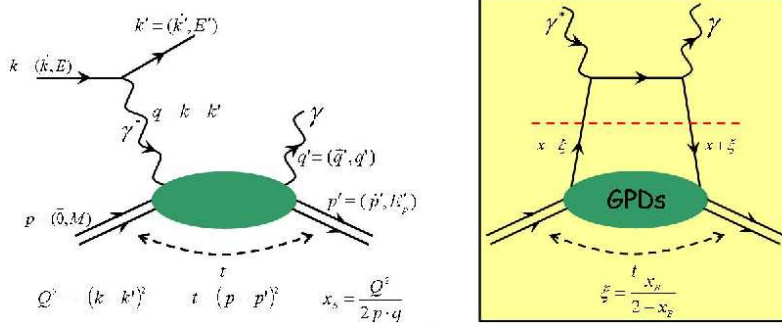


Figure 2. DVCS representation: kinematic variables (left), and handbag diagram (right).

corresponding to the photon-quark interaction and an unknown soft part related to GPDs.

In addition to the DVCS amplitude, the cross section for leptonproduction of photons gets contributions from the Bethe-Heitler (BH) process where the real photon is emitted by the initial or final lepton, leading to

$$\frac{d^5\sigma}{dQ^2 dx_B dt d\phi_e d\varphi} = \mathcal{T}_{BH}^2 + |\mathcal{T}_{DVCS}|^2 + 2 \mathcal{T}_{BH} \Re\{\mathcal{T}_{DVCS}\} \quad (5)$$

where  $\varphi$  is the out-of-plane angle between the leptonic and hadronic planes. Though the BH amplitude dominates the cross section at JLab energies, it is a completely known process exactly calculable from the nucleon electromagnetic form factors. Polarization degrees of freedom help to overcome this problem from their sensitivity to the interference between the BH and DVCS amplitudes. For instance, the polarized cross section difference for opposite beam helicities can be expressed as [15, 16]

$$\begin{aligned} \frac{d^5\Delta\sigma}{dQ^2 dx_B dt d\phi_e d\varphi} &= \frac{1}{2} \left[ \frac{d^5\vec{\sigma}}{dQ^2 dx_B dt d\phi_e d\varphi} - \frac{d^5\overleftarrow{\sigma}}{dQ^2 dx_B dt d\phi_e d\varphi} \right] \\ &= \mathcal{T}_{BH} \Im\{\mathcal{T}_{DVCS}\} + \Re\{\mathcal{T}_{DVCS}\} \Im\{\mathcal{T}_{DVCS}\} \end{aligned} \quad (6)$$

where the imaginary part of the DVCS amplitude appears now linearly instead of quadratically, and magnified by the BH amplitude. These observables can be decomposed in terms of harmonics with respect to  $\varphi$  [17] leading, in the twist-3 approximation, to

$$\begin{aligned} \frac{d^5\Delta\sigma}{dQ^2 dx_B dt d\phi_e d\varphi} &= \Gamma_2(x_B, Q^2, t) s_1^{DVCS} \sin(\varphi) \\ &+ \frac{\Gamma_3(x_B, Q^2, t)}{P_1(\varphi)P_2(\varphi)} [s_1^I \sin(\varphi) + s_2^I \sin(2\varphi)] \end{aligned} \quad (7)$$

where  $\Gamma_i$  are kinematical factors and  $P_i$  are the BH propagators. In this expression,  $s_1^{DVCS}$  and  $s_2^I$  are twist-3 coefficients while  $s_1^I = k \Im m\{C^I(\mathcal{F})\}$  is a twist-2 coefficient directly linked to the linear combination of GPDs

$$C^I(\mathcal{F}) = F_1 \mathcal{H} + \frac{x_B}{2 - x_B} (F_1 + F_2) \tilde{\mathcal{H}} - \frac{t}{4M^2} F_2 \mathcal{E} \quad (8)$$

with for example

$$\begin{aligned} \mathcal{H} &= \sum_q \mathcal{P} \int_{-1}^{+1} dx \left( \frac{1}{x - \xi} + \frac{1}{x + \xi} \right) H^q(x, \xi, t) \\ &- i\pi \sum_q e_q^2 [H^q(\xi, \xi, t) - H^q(-\xi, \xi, t)] \end{aligned} \quad (9)$$

$e_q$  being the electric charge of the considered quark in unit of the elementary charge. The dominance of a twist-2 contribution to the cross section is a strong indication for factorization and enables a GPD based interpretation.

#### 4 Recent Results from Jefferson Laboratory

The first DVCS candidate signal was reported by the H1 collaboration [18] from a deviation observed in the photon electroproduction cross section as compared to the BH cross section: in the H1 energy range, the DVCS process dominates the cross section. At smaller energy, the interference between the DVCS and the BH amplitudes was observed successively at HERMES [19] and CLAS [20] as a characteristic  $\sin(\varphi)$  dependence of the relative beam spin asymmetry. These last experiments are strong evidences of the existence of a DVCS signal but do not tell about the reliability of a GPD based interpretation whose prerequisite is an experimental proof of the factorization of the cross section. This motivates in part the experimental program at JLab.

##### 4.1 The E00-110 $p(\vec{e}, e'\gamma)p$ and E03-106 $n(\vec{e}, e'\gamma)n$ Hall A Experiments

The E00-110 [21] and E03-106 [22] experiments have been taking data successively on hydrogen and deuterium in the hall A of JLab, investigating different issues of the DVCS process: in the former case, the test of handbag dominance in the valence region ( $x_B = 0.36$ ) between  $Q^2 = 1.9 \text{ GeV}^2$  and  $2.3 \text{ GeV}^2$  is under concern while the latter measurement is an exploratory attempt to access  $E$ , the least known and constrained GPD which directly enters Ji's sum rule (eq. 4).

A specific experimental setup (fig. 3) has been instrumented which involves a new reaction chamber (RC), a PbF<sub>2</sub> electromagnetic calorimeter (EC), a recoil detector (RD), and customized electronics and data acquisition [23]: the new RC is optimized in thickness and features a larger exit beam pipe, reducing the otherwise very high rate of Møller electrons; the Čerenkov sensitive material of the EC insures the rapidity of the delivered signal and a reduced sensitivity

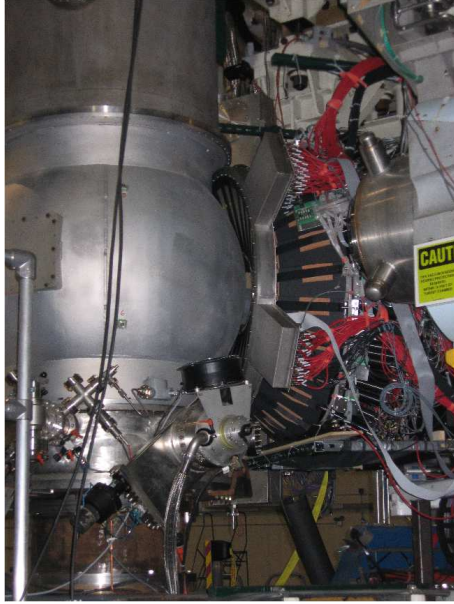


Figure 3. The E00-110 and E03-106 experimental setup in the Hall A of JLab.

to hadronic background; the RD allows to check the exclusivity of the reaction selection; the read-out electronics based on Analog Ring Samplers [24] resolves the pile-up of signals separated from at least 5 ns. These many features allow the detector operation in the highly hostile environment of an electromagnetic facility: current luminosities of  $4 \times 10^{37} \text{ cm}^{-2} \cdot \text{s}^{-1}$  were achieved during deuterium data taking.

From the measurement of beam helicity dependent cross sections for photon electroproduction, the  $\varphi$  harmonic structure of the sum and the difference of polarized cross sections for opposite beam helicities (Sec. 3) is investigated neglecting contributions of the squared DVCS amplitude [25]. Experimental results for the proton case [26] are reported on fig. 4: the twist-2 ( $\Im m\{C^I(\mathcal{F})\}$ ) and twist-3 ( $\Im m\{C^I(\mathcal{F}^{eff})\}$ ) harmonics are essentially  $Q^2$  independent; thanks to different kinematical factors the twist-3 contribution to the cross section turns out to be small; the general trend of the  $t$  dependence of the different harmonics is consistent with a GPD based calculation while the exact magnitude is not reproduced. These features are evidences of the factorization of the cross section at  $Q^2$  as small as  $2 \text{ GeV}^2$  and support the prediction of perturbative Quantum Chromo-Dynamics scaling in DVCS [6, 7]. This legitimates a GPD based interpretation and this experiment provides for the first time a model-independent measurement of linear combinations of GPDs and GPDs integrals.

Because of the cancellation between the  $u$  and  $d$  quarks in  $\tilde{H}$  and following

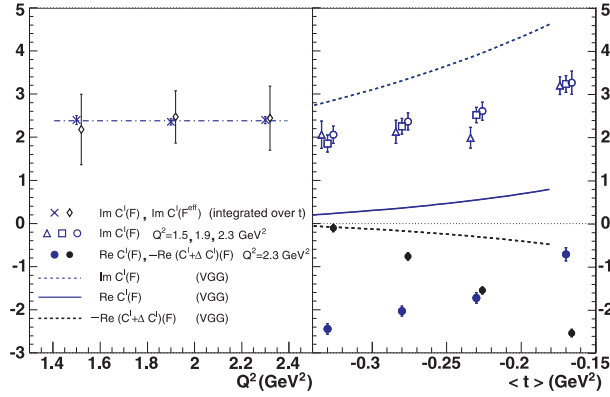


Figure 4.  $Q^2$  and  $t$  dependences of the harmonic coefficients extracted from E00-110 measurements [26]; curves labelled VGG are twist-2 calculations neglecting the contribution of the GPD  $E$  [27–29].

$F_1(t) \approx 0$  at small  $t$ , the DVCS process on a neutron target turns out to be a unique tool to access  $E$  (eq. 8). The  $n(\vec{e}, e'\gamma)n$  polarized cross sections are deduced via the subtraction of the proton yield measured with  $p(\vec{e}, e'\gamma)p$  from the  $D(\vec{e}, e'\gamma)X$  yield where the residual system  $X$  can be either a nucleon or a deuteron [30]. The deconvolution of these two contributions is insured by their dynamical separation  $\Delta M_X^2 = t/2$  in the missing mass spectra. It should be also noticed that the coherent deuterium channel is expected to be small and rapidly decreasing with  $t$  following the electromagnetic form factors dependence. These features allow for a reliable extraction of the neutron DVCS cross section [31].

#### 4.2 The E01-113/E06-003 $p(\vec{e}, e'\gamma)$ Hall B Experiment

Similar measurements with an unpolarized hydrogen target [32] have been recently performed in hall B with the aim of studying GPDs from both electroproduction of photons and mesons. Thanks to the acceptance of the CLAS detector [33], a large phase space in  $(Q^2, x_B, t)$  is explored in terms of relative beam spin asymmetries (BSA) and cross sections.

This first dedicated DVCS experiment in Hall B required additions to CLAS: an electromagnetic calorimeter consisting of 424  $\text{PbWO}_4$  crystals is installed in the central part of CLAS for the  $\gamma$  detection between 4 and 16 degrees; in order to allow operation of this device, a superconducting solenoidal magnet placed prior to the calorimeter confines low energy Møller electrons in the beam pipe [34]. The selection of the DVCS process is insured by the triple coincidence detection of the scattered electron, the recoil proton, and the produced real photon.

It should be noticed that while BSA are in principle easier to measure than cross sections, their GPD interpretation is basically more difficult. The E00-110 experiment shows that in the JLab energy range, the BSA  $\varphi$  structure is more

complex than the simple  $\sin(\varphi)$  assumed in earlier experiments. Consequently, the harmonic coefficients can only be extracted through iterative procedures involving some GPD parametrizations, meaning that BSA interpretation in terms of GPDs is model dependent.

#### 4.3 The E05-114 $\vec{p}(\vec{e}, e'\gamma p)$ Hall B Experiment

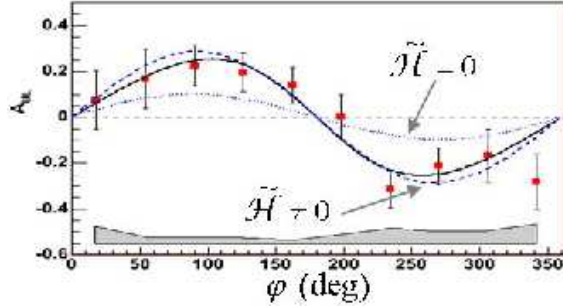


Figure 5. Target spin asymmetry measured by the CLAS collaboration on a longitudinally polarized hydrogen target [35]. The dashed and dotted curves are model predictions showing the sensitivity to  $\tilde{\mathcal{H}}$ , and the solid curve is a fit to the data neglecting the  $\varphi$  dependence of the denominator.

Beam polarization observables are not unique tools in DVCS to reveal the GPD content of the nucleon. There exists indeed a complete set of observables involving beam and/or target polarization: each observable gives access to a different linear combination of GPDs, and at least four different observables are required to unravel GPDs. For instance, the difference between polarized cross sections for opposite longitudinal polarization of a proton target measures the combination

$$C_{LP}^I(\mathcal{F}) = \frac{x_B}{2-x_B}(F_1 + F_2) \left( \mathcal{H} + \frac{x_B}{2}\mathcal{E} \right) + F_1\tilde{\mathcal{H}} - \frac{x_B}{2-x_B} \left( \frac{x_B}{2}F_1 + \frac{t}{4M^2}F_2 \right) \tilde{\mathcal{E}} \quad (10)$$

where  $C_{LP}^I(\mathcal{F})$  plays an equivalent role to  $C^I(\mathcal{F})$  of eq. 8. Because of the kinematical factors weighting each GPD, the combination of eq. 10 is expected to be sensitive to  $\tilde{\mathcal{H}}$ . This feature was observed in an experiment performed in the Hall B of JLab where the target spin asymmetry (TSA) of the DVCS process was measured for a longitudinally polarized hydrogen target [35]. The results reported on fig. 5 show that a GPD based model taking into account the contribution of  $\tilde{\mathcal{H}}$  is more likely able to reproduce the data than the same calculation neglecting this contribution. This observation motivates the E05-114 dedicated experiment [36] which will investigate the TSA and the double spin asymmetry (DSA) with the CLAS detector over a large phase space in the variables



$(Q^2, x_B, t)$ : the TSA will measure  $\Im m\{C_{LP}^I(\mathcal{F})\}$  while the DSA involving beam and target polarizations will measure  $\Re e\{C_{LP}^I(\mathcal{F})\}$ .

## 5 Perspectives

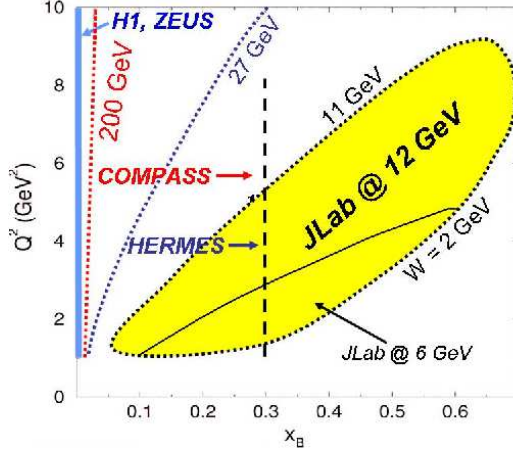


Figure 6. Experimental phase space relative to the different programs investigating GPDs.

The fundamental character of the GPD framework motivates several experimental programs at major lepton facilities whose combination provides a systematic mapping of these distributions (fig. 6). Depending on the available beam energy, different aspects of the nucleon structure can be investigated: H1 and ZEUS experiments at DESY probe the GPDs in the very small  $x_B$  region relevant for the gluon content of the nucleon, HERMES [37] at DESY and COMPASS [38,39] at CERN extend their investigation up to the valence quark region, and the energy upgrade of JLab [40,41] allows to access the high  $x_B$  domain. The remarkable complementarity between these different experiments will provide a comprehensive picture of the nucleon structure, including the flavor decomposition of GPDs which is achieved from deeply virtual meson production and/or proton and neutron DVCS.

## 6 Conclusions

The study of nucleon structure is living very exciting moments. The factorization of the DVCS cross section on the proton was established at JLab, opening access to GPDs. A worldwide very promising experimental investigation of the GPD framework is starting. In a near future, the dedicated program at JLab and

COMPASS will deliver unprecedented information on the quark and gluon content of the nucleon, hopefully unraveling the nucleon spin puzzle and the quark confinement.

### Acknowledgments

I would like to thank the organizers of the XXVth International Workshop on Nuclear Theory for their invitation and warm hospitality at Rila Mountains.

This work was supported in part by the U.S. Department of Energy (DOE) contract DOE-AC05-06OR23177 under which the Jefferson Science Associates, LLC, operates the Thomas Jefferson National Accelerator Facility, the National Science Foundation, the French Atomic Energy Commission and National Center of Scientific Research.

### References

- [1] R. Hofstadter, R.W. McAllister, *Phys. Rev.* **98** (1955) 217.
- [2] M. Breidenbach, J.I. Friedman, H.W. Kendall, E.D. Bloom, D.H. Coward, H. DeStaebler, J. Drees, L.W. Mo, R.W. Taylor, *Phys. Rev. Lett.* **23** (1969) 935.
- [3] J. Ashman *et al.*, *Phys. Lett.* **B 206** (1988) 364; *Nucl. Phys.* **B 328** (1989) 1.
- [4] S. Ageev *et al.*, *Phys. Lett.* **B 633** (2006) 25.
- [5] D. Müller, D. Robaschick, B. Geyer, F.M. Dittes, J. Hořejši, *Fortschr. Phys.* **42** (1994) 101.
- [6] A.V. Radyushkin, *Phys. Rev.* **D 56** (1997) 5524.
- [7] X. Ji, *Phys. Rev. Lett.* **78** (1997) 610.
- [8] M. Burkardt, *Phys. Rev.* **D 62** (2000) 071503.
- [9] J.P. Ralston, B. Pire, *Phys. Rev.* **D 66** (2002) 111501.
- [10] M. Diehl, *Eur. Phys. Jour.* **C 25** (2002) 223.
- [11] A.V. Belitsky, D. Müller, *Nucl. Phys.* **A 711** (2002) 118c.
- [12] M. Diehl, *Phys. Rep.* **388** (2003) 41.
- [13] X. Ji, J. Osborne, *Phys. Rev.* **D 58** (1998) 094018.
- [14] J.C. Collins, A. Freund, *Phys. Rev.* **D 59** (1999) 074009.
- [15] P.A.M. Guichon, M. Vanderhaeghen, *Prog. Part. Nucl. Phys.* **41** (1998) 125.
- [16] I. Bensafa, Doctorat Thesis, Université Blaise Pascal, Clermont-Ferrand (France), **DU 1647** (2006).
- [17] A.V. Belitsky, D. Müller, A. Kirchner, *Nucl. Phys.* **B 629** (2002) 323.
- [18] C. Adloff *et al.*, *Phys. Lett.* **B 517** (2001) 45.
- [19] A. Airapetian *et al.*, *Phys. Rev. Lett.* **87** (2001) 182001.
- [20] S. Stepanyan *et al.*, *Phys. Rev. Lett.* **87** (2001) 182002.
- [21] P.Y. Bertin, C.E. Hyde-Wright, R. Ransome, F. Sabatié *et al.*, *JLab Proposal* **E00-110** (2000).
- [22] P.Y. Bertin, C.E. Hyde-Wright, F. Sabatié, E. Voutier *et al.*, *JLab Proposal* **E03-106** (2003).
- [23] A. Camsonne, Doctorat Thesis, Université Blaise Pascal, Clermont-Ferrand (France), 2005.

- [24] D. Lachartre, F. Feinstein, *Nucl. Inst. Meth.* **A 422** (2000) 99.
- [25] C. Muñoz Camacho, Doctorat Thesis, Université Pierre et Marie Curie, Paris (France), **DAPNIA-05-17-T** (2005).
- [26] C. Muñoz Camacho, A. Camsonne, M. Mazouz, C. Ferdi, G. Gavalian, E. Kuchina *et al.*, *arXiv:nucl-ex/0607029* (2006).
- [27] M. Vanderhaeghen, P.A.M. Guichon, M. Guidal, *Phys. Rev.* **D 60** (1999) 094017.
- [28] K. Goetze, M.V. Polyakov, M. Vanderhaeghen, *Prog. Part. Nucl. Phys.* **47** (2001) 401.
- [29] M. Guidal, M.V. Polyakov, A.V. Radyushkin, M. Vanderhaeghen, *Phys. Rev.* **D 72** (2005) 054013.
- [30] M. Mazouz, Proc. of the  $V^{th}$  *International Conference on Perspectives in Hadronic Physics*, Edts. C. Ciofi degli Atti and D. Treleani, Trieste (Italy), May 22-26, 2006.
- [31] M. Mazouz, Doctorat Thesis, Université Joseph Fourier, Grenoble (France), 2006.
- [32] V. Burkert, L. Elouadrhiri, M. Garçon, R. Niyazov, S. Stepanyan *et al.*, *JLab Proposal* **E01-113** (2001); *JLab Proposal* **E06-003** (2006).
- [33] B.A. Mecking *et al.*, *Nucl. Inst. Meth.* **A 503** (2003) 513.
- [34] F.-X. Girod, Cont. to the *GPD2006 Workshop*, <http://gpd.gla.ac.uk/gpd2006>, Trento (Italy), June 5-9, (2006).
- [35] S. Chen *et al.*, *arXiv:hep-ex/0605012* (2006).
- [36] A. Biselli, L. Elouadrhiri, K. Joo, S. Nicolai *et al.*, *JLab Proposal* **E05-114** (2005).
- [37] W.-D. Nowak, Cont. to the *GPD2006 Workshop*, <http://gpd.gla.ac.uk/gpd2006>, Trento (Italy), June 5-9, (2006).
- [38] COMPASS Collaboration, *Expression of Interest* **CERN-SPSC-2005-007 SPSC-EOI-005** (2005).
- [39] E. Burtin, Cont. to the *GPD2006 Workshop*, <http://gpd.gla.ac.uk/gpd2006>, Trento (Italy), June 5-9, (2006).
- [40] C.E. Hyde-Wright, B. Michel, C. Muñoz Camacho, J. Roche *et al.*, *JLab Proposal* **PR12-06-114** (2006).
- [41] A. Biselli, H. Egiyan, L. Elouadrhiri, M. Holtrop, D. Ireland, W. Kim, F. Sabatié *et al.*, *JLab Proposal* **PR12-06-119** (2006).